Low-Cost Hand Vein Pattern Recognition

Distler, Marion; Jensen, Sebastian H. Nesgaard; Myrtue, Niels G.; Petitimbert, Claire; Nasrollahi, Kamal; Moeslund, Thomas B.

Publication date:
2011

Document Version
Publisher's PDF, also known as Version of record

Low-Cost Hand Vein Pattern Recognition

Marion Distler, Sebastian Jensen, Niels G. Myrtue, Claire Petitimbert, Kamal Nasrollahi, and Thomas B. Moeslund
Laboratory of Computer Vision and Media Technology,
Aalborg University, Aalborg, Denmark

***Abstract*—Identification based on hand vein pattern is an interesting branch of biometric recognition that is enjoying increasingly attention among the researchers in the recent decade. However, despite the fact the most of the developed commercial systems for this purpose are expensive, their false acceptance ratios are not zero. Therefore, using them for identification purposes can be crucial if they mistakenly accept an imposter (even with a very low probability). The current work proposes a very low-cost hand vein pattern recognition system using a simple modified webcam. The system introduces a blob removal algorithm for enhancing the results of the segmentation and uses a modified version of Hausdorff distance for feature matching for the recognition purposes. Experimental results show that the system can achieve a zero false acceptance ratio while keeping the true acceptance rate in an acceptable level.**

Keywords- Pattern Recognition; Hand Vein; Biometrics; Infrared Imaging.

I. INTRODUCTION

Biometric recognition systems are widely employed nowadays for identification purposes in different areas including access control applications. Depending on the features of the environment in which the biometric recognition system is employed, like the level of the security, different factors can be taken into account for choosing the right biometrics among the available options: face, ear, iris, retina, fingerprint, hand vein pattern, etc. Among others, hand vein patterns are proven to have all the features of a good biometric: universality, distinctively, collectability and permanence. However, due to the fact that most hand vein recognition systems use expensive sensors for imaging the vein patterns, their employment is not as wide as other biometrics like face, though they are well studied [1-7]. Furthermore, most of the recognition systems based on hand vein patterns have to compromise between the end cost and the false acceptance rate of the system.

Miura et al. [2] use infrared imaging to capture the vein pattern images. These images contains not only the vein pattern but also irregular shading produced by the various thicknesses of the finger bones and muscles. Therefore, they employee repeated line tracking for extracting the vein patterns from the unclear images obtained by the infrared. Kumar and Prathyusha [4] use the triangulation of hand vein images and simultaneous extraction of knuckle shape information for identification purposes. They use the knuckle tips as key points for the image normalization and extraction of region of interest. Zhao et al. [5] propose a denoising algorithm using wavelets thresholding based on Besov norm regularization. This algorithm could remove the high noise while do not hurt the contrast between the vein patterns and the non-vein areas. Wang and Leedham [6] use expensive thermal sensors to capture the vein patterns. Though, most of the developed systems for vein pattern recognition in the literature have achieved an acceptable true acceptance rate, they mostly use some expensive equipment while their false acceptance rates are not zero. The proposed system in this paper develops a very low price hand vein pattern identification system using a modified simple webcam which achieves zero false acceptance rate while keeps the true acceptance rate of the system reasonably high. This webcam is accompanied with some near infrared emitter. The veins absorb these signals more compared to their surrounding skin areas and will consequently be more visible.

The rest of this paper is organized as follows. The low-cost imaging setup developed for this work is described in the next section. Section III gives the details of the different parts of the proposed system. The experimental results are discussed in section IV and finally the paper is drawn to a conclusion in section V.

In order to develop a very low cost system which has the ability to capture the vein patterns, a simple Logitech webcam has been modified as follows. First of all, the internal near infrared filter of the camera has been removed. Then, the visible light is blocked by attaching a Kodak Gold ISO 200 film negative to the lens of the camera. Furthermore, to make sure that the camera can capture the vein patterns four infrared light emitting diodes have been used. The diodes are placed in a box which contains the camera (Figure 1(left)). They are positioned in a way which removes the shadows caused by small level differences on the hand's surface.

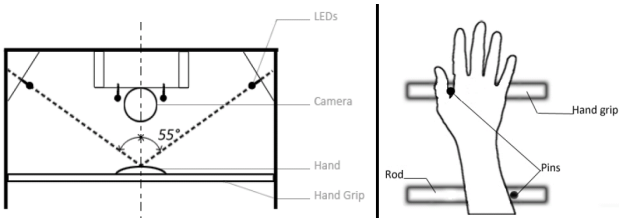

Figure 1. Left: capturing setup, right: hand constraint points.

Inside the imaging box, a hand grip and a rod are used to make sure that the region of interest of the hand is extracted carefully by the system. To prevent any movements during the imaging, two pins have been added: one on the hand grip, the other on the rod (Figure 1(right)). Having extracted the region of the interest from the subject's hand it is fed to the proposed algorithm which is described in the next section.

Input Image	Preprocessing	Segmentation	Post-Processing	Feature Extraction	Recognition
	Smoothing, Noise removal Contrast Enhancement	Repeated Line Tracking Laplacian of Gaussian Direction Based Vascular Pattern Extraction	Morphology Blob Removal	Thinning	Modified Hausdorff Distance

Figure 2. The block diagram of the proposed method.

II. THE PROPOSED ALGORITHM

The block diagram of the proposed system is shown in Figure 2. Having extracted the region of interested in the captured image it is first converted into a gray image. Then, in the preprocessing block a smoothing filter followed by a contract enhancement algorithm are applied to the extracted region. Next, the vein areas are segmented from the non-vein areas in the segmentation block. In the post-processing step a morphological operation followed by a blob removal algorithm are applied. Finally, the feature extraction and the recognition are performed in the last two blocks of the system.

The following subsections describe the details of each of the above mentioned steps. Since the segmentation block is one of the most important blocks in such a system, we have studied different options for this block. These options are all shown in the block diagram of the system in Figure 2. However, the employed method for this block has been highlighted among the available options the block diagram of the system.

A. Preprocessing

Since the images are captured by a low-cost modified webcam a considerable amount of noise is usually present. Therefore, as the first step of the preprocessing, a smoothing and noise removal step is applied. To remove the effect of the noise a Gaussian filter is used. Then, a median filter is employed to remove noises resulted from the presence of hairs on the back of the hand.

Furthermore, since the vein patterns can be faint, the second step of the preprocessing makes them more visible. To do so, a histogram stretching algorithm is used to add contrast between the veins and the background. Figure 3 shows an image captured by the imaging device explained in the previous section and its preprocessed counterpart. It is obvious that the vein patterns are more visible in the preprocessed image than in the input image and the amount of noise is reduced. Therefore, it is fed to the next step of the system for performing the segmentation.

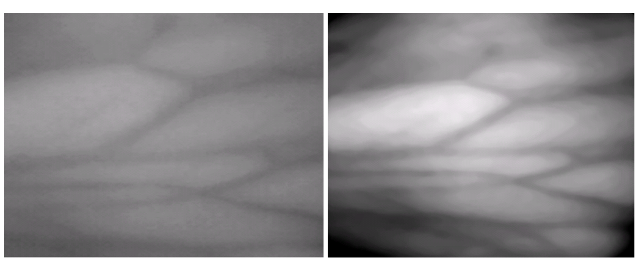

Figure 3. An input image (left) and its preprocessed counterpart (right).

B. Segmentation

The segmentation separates the vein pixels from the non-vein ones. Due to the importance of this step in the overall performance of the system, several segmentation algorithms have been implemented here, including: Repeated Line Tracking (RLT) [2], Laplacian of Gauusian (LoG), and Direction Based Vascular Pattern Extraction (DBVPE) [3]. Figure 4 shows four different preprocessed input images and their segmented counterparts obtained by these three segmentation methods.

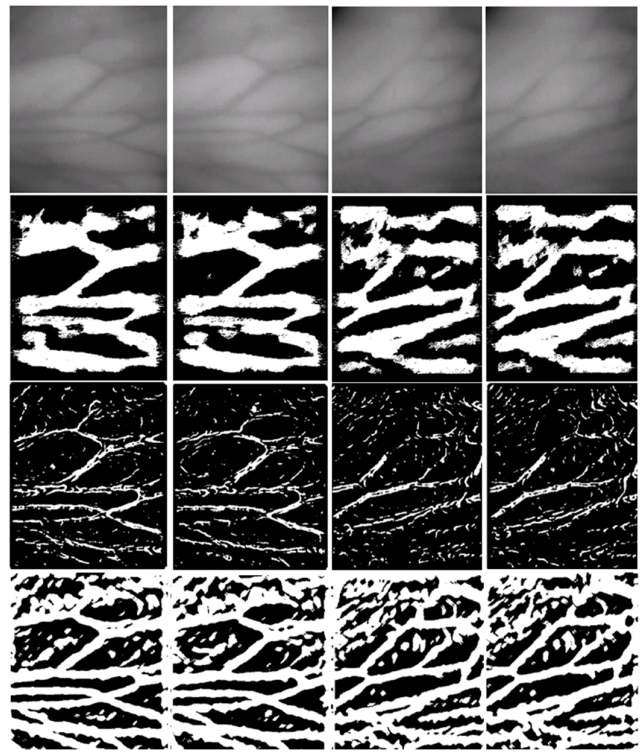

Figure 4. From top, first row: four preprocessed input images and their segmented counterparts obtained by: RLT (second row), LoG (third row), and DBVPE (last row).

From Figure 4 (which has been observed for many other sample images) it seems that the best segmentation method for the purposes of the current work with the highest precision is DBVPE, as it produces a fairly stable matching segmented pattern for all the test figures (last row of Figure 4). Though, the images contain some noise, most of it can be removed via the post-processing methods described in the next section. In most of the images, the LoG edge detection seems to be incapable of producing an accurate pattern (third image of the third row of Figure 4). On the other hand, RLT seems to have the opposite problem, as it produces quite bulky patterns that seem to merge close veins and shadows together. Regarding stability the RLT seems to be a bit more stable than the DBVPE, as the latter method is slightly vulnerable to noise on the edges of the image.

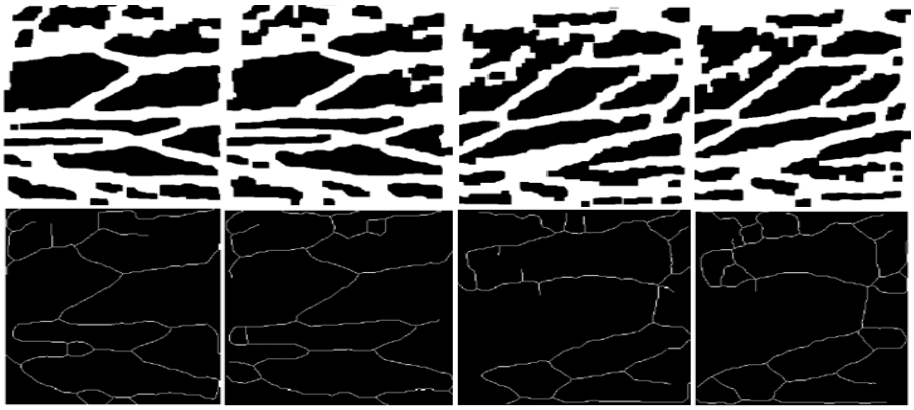

Figure 5. The results of applying the post-processing steps to the images of the last row of Figure 4 (top) and their thinned counterparts (bottom).

However, as the precision is preferred to the stability it is decided to use the ALT.

The better results of DBVPE are due to the fact that the proposed system combines the original DBVPE algorithm [3] with a local adaptive thresholding algorithm. The local adaptive thresholds for any window of size $w \times w$ in the input image are found using [xx-9]:

$$t(x,y) = \frac{1}{w^2} \sum_{i=x-\frac{w}{2}}^{x+\frac{w}{2}} \sum_{j=y-\frac{w}{2}}^{y+\frac{w}{2}} f(i,j) \qquad (1)$$

where t is the local threshold for the current window and f is the pixel's value of the image in the location of *(i, j)*.

Having segmented the preprocessed input image in the previous section, it is fed to the next step to further remove its noise.

C. Post-processing

The post-processing block composes of two steps. First morphological operations, an opening followed by a closing, are applied to the segmented image. Though, the morphological operations can remove most of the noise, it is likely to leave some small blobs in image. Therefore, a small blob removal algorithm has been introduced here as follows.

The algorithm works by iterating through the image, searching for white pixels. When a white pixel is found, the algorithm searches the four adjacent pixels for additional white pixels and adds them to a list. Next, the first pixel in the list is used as a new starting point and its four neighbors are searched. This is repeated until all white pixels in the blob have been found. Meanwhile, the algorithm keeps track of the size of the current blob. When all blobs in the image have been identified, the ones with a size below a specified fraction of the largest blob are removed.

The results of applying the above two post-processing steps to the images of the last row of Figure 4 are shown in Figure 5(left). It can be seen that in addition to removing the noise the small blobs are removed as well.

Having extracted the vein patterns from the segmented images, in the next section they will be converted to suitable shapes to be used as features.

D. Feature Extraction using Thinning

Thinning methods try to extract the skeleton of the vein pattern. The skeleton is a binary representation of the pattern with only one pixel wide. To extract the skeleton, the method explained in [8] has been used. This method iteratively deletes layers of pixels (in a parallel way) on the boundary of a pattern until only the skeleton remains, without shortening it or breaking it apart. Each iteration is divided into sub-iterations in which only a subset of contour pixels are considered for removal. At the end of each sub-iteration, the remaining image is updated for the next sub-iteration. It is common to use a combination of four sub-iterations, in which each type of contour point (top, bottom, right, left) is removed in each sub-iteration, with two other sub-iterations, which could be for example in one sub-iteration deleting the top and right and in the other deleting the rest. Even if this algorithm produces a good skeleton of the vein pattern, the result can be improved by reducing the number of unnecessary small branches. The algorithm used to do so is called pruning. The reader is motivated to see [8] for more details on these algorithms. Figure 5(right) shows the result of applying this thinning algorithm to the image in Figure 5(left).

E. Recognition using Modified Hausdorff Distance (MHD)

Having extracted the thinned image from the post-processed image, we use the Hausdorff distance to feature matching. The Hausdorff distance is a measure of how far two sets of points are from each other. The Hausdorff distance here is defined as:

$$H(A,B) = max(h(A,B), h(B,A)) \qquad (2)$$

where A and B are the sets of points of the thinned images in the gallery and the probe, and h is defined as:

$$h(A,B) = sup_{a \in A}(inf_{b \in B}(d(a,b))) \qquad (3)$$

where a and b are the points in A and B and d is the Euclidian distance between a and b. The $inf_{b \in B}(d(a,b))$ operator finds the minimal distance from B to any given point in A. Then, the maximum of the minimal distance from B to A is found by $sup_{a \in A}$.

In theory, the Hausdorff distance gives an accurate measure of the difference between two images. In practice for vein pattern recognition, if thinning and pruning have already been applied to the binary image, Hausdorff distance does not give good enough results for recognition. Indeed, occasional branches randomly appear and disappear after segmentation and post-processing of different images of the same pattern. This is problematic because it yields a high Hausdorff distance between the images, even though the rest of the patterns are identical. To make the distance measure less sensitive to noise, an average of the minimum distance is used instead, which for a set of points is defined as:

$$h_{average}(A,B) = \frac{1}{n}\sum_{i=0}^{n} inf_{b\in B}(d(a,b)) \tag{4}$$

It is of course necessary to limit the number of times that each individual distance can contribute in the calculations. Here this limit is set to 20, as it gives the best result in practice. Capping each contribution reduces the amount by which a single faulty branch can change the average distance. This makes the distance measure more resistant to noise, while still being reliable. Further details on the recognition method are given in the following section.

III. Experimental Results

The results of the proposed system in this paper have been evaluated using a database containing hand images of 27 people mostly from an age group of 19-25, mostly male and non-Caucasians. 20 persons out of the 27 people are involved in both the training and testing of the system while the 7 remaining persons are only involved in validation of the system. The gallery of the database contains four thinned images of the vein patterns of the right hand of each person. Having an input test image, its thinned version is first calculated. Then, its average distance from all the images in all the classes of the database is calculated using the modified Hausdorff distance. Finally, if the distance between the input image and its closest class in the database is smaller than a predefined threshold, the input is identified as a member of that class. Table I shows the results of employing different threshold values.

TABLE I. True and False Acceptance Rates of the System vs. The Threshold of the Recognition

Threshold	*True Acceptance Rate*	*False Rejection Rate*	*False Acceptance Rate*
9	0.75	0.25	0
9.5	0.83	0.16	0.004
9.76	0.85	0.14	0.02
10.14	0.90	0.08	0.15
10.5	0.93	0.03	0.2

The different threshold values are found during the training of the system. Depending on the expectations from the system, some compromise should be taken into account between the true acceptance rate and false acceptance rate of the system. Figure 6 shows the ROC curve of the system for illustrating this compromise.

Table II compares the proposed system against some of the similar systems in the literature using false acceptance and rejection rates. It is shown that our system can get a zero false acceptance rate while its false rejection rate is indeed comparable with the other systems. This is despite of the fact that the cost of our system is much lower than the similar ones.

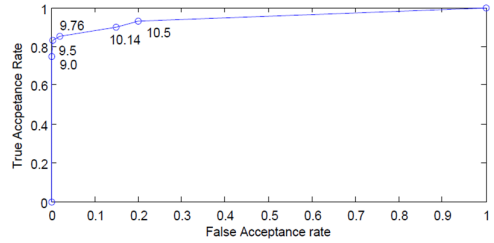

Figure 6. The ROC curve of the proposed system.

TABLE II. The Proposed System vs. Similar Systems

System	*False Rejection Rate*	*False Acceptance Rate*
Miura et al [2]	0	0.10
Lin and Fan [3]	0.15	0.35
The Proposed System	0.25	0

IV. Conclusion

By modifying a very low-price webcam, the proposed system in this paper constructs a simple imaging setup for vein pattern recognition. The processing algorithm of the system composes different steps including: preprocessing, segmentation, post-processing, feature extraction and finally recognition. Adaptive local thresholding using direction based vascular pattern extraction has been used for segmentation and a modified version of Hausdorff distance for the recognition. The experimental results of the system show that the system can achieve a zero false acceptance rate while its true acceptance rate is acceptably high. This is indeed the goal of the system as a lower true acceptance rate is less risky than a higher false acceptance rate. Because a person who is wrongly rejected can simply try again, while the risk of accepting an imposter can be crucial.

References

[1] L. Wang, G. Leedham, and D. S.-Y. Cho, “Minutiae feature analysis for infrared hand vein pattern biometrics,” Pattern Recognition, vol. 41, pp. 920-929, 2008.

[2] N. Miura, A. Nagasaka, and T. Miyatake, “Feature extraction of finger-vein patterns based on repeated line tracking and its application to personal identification,” Machine Vision and Applications, vol. 15, pp. 194-203, 2004.

[3] S. K. Im, H. S. Choi, and S.-W. Kim., “A direction-based vascular pattern extraction algorithm for hand vascular pattern verication,” ETRI journal, vol. 5, no. 2, pp.101-108, 2003.

[4] A. Kumar and K. V. Prathyusha, “Personal authentication using hand vein triangulation and knuckle shape,” IEEE Transactions on Image Processing, no. 38, pp.2127-2136, 2009.

[5] S. Zhao, Y.-D. Wand, and Y.-H. Wang, “Biometric identification based on low-quality hand vein pattern images," in Seventh International Conference on Machine Learning and Cybermetrics, Kunming, 2008.

[6] L. Wang and G. Leedham, “A thermal hand vein pattern verification system,” Lecture Notes in Computer Science, pp. 58-65, 2005.

[7] H. Zhang and D. Hu, "A Palm Vein Recognition System," in IEEE International Conference on Intelligent Computation Technology and Automation, China, 2010.

[8] L. Lam, S. Lee, and C. Suen, “Thinning methodologies-a comprehensive survey,” IEEE Transactions on Pattern Analysis and Machine Intelligence, vol. 14, no. 9, pp. 869-879, September 2002.